The development of an axisymmetric curved turbulent wall jet

D. G. Gregory-Smith
School of Engineering and Applied Science, University of Durham, Durham, UK

M. J. Hawkins
ICI Chemicals & Polymers Ltd., Teesside Operations, Billingham, Cleveland, UK

An experimental study has been carried out of the low speed Coanda wall jet with both streamwise and axisymmetric curvature. A single component laser Doppler technique was used, and by taking several orientations at a given point, values of the three mean velocities and five of the six Reynolds stresses were obtained. The lateral divergence and convex streamwise curvature both enhanced the turbulence in the outer part of the jet compared with a plane two-dimensional wall jet. The inner layer exhibited a large separation of the positions of maximum velocity and zero shear stress. It was found that the streamwise mean velocity profile became established very rapidly downstream of the slot exit. The profile appeared fairly similar at later downstream positions, but the mean radial velocity and turbulence parameters showed the expected nonself preservation of the flow. Removal of the streamwise curvature resulted in a general return of the jet conditions toward those expected of a plane wall jet. The range and accuracy of the data may be used for developing turbulence models and computational techniques for this type of flow.

Keywords: Coanda flow; turbulent jets; curved jets; laser Doppler anemometry

Introduction

The effect whereby a jet of fluid attaches itself to an adjacent curved surface is often termed the Coanda effect. Bradshaw,[1] in discussing the effect, identified various phenomena, one of which was the effect of streamline curvature in producing enhanced turbulence and entrainment through the extra rate of strain. A plane jet flowing radially outward, as studied by Bakke,[2] also provides an extra rate of strain through the divergence of the flow. A particular application of these two phenomena is to the Coanda flare, developed by the petroleum industry for burning waste gases. As described by Wilkins et al.,[3] a jet of gas emerges from a slot at the base of an axisymmetric tulip-shaped body, illustrated in Figure 1. The divergence and curvature of the jet cause rapid entrainment of ambient air, and hence good premixing, leading to efficient combustion. Combustion is initiated near the top of the body, so the flow around the curved part is largely uninfluenced by combustion.

Bradshaw[1] has indicated that the effect of an extra rate of strain on the turbulent Reynolds stresses is of the order of ten times that suggested directly by the extra terms in the stress transport equations. In other words, an extra strain rate changes the Reynolds stresses for the turbulent flow by about ten times as much as it changes the viscous stresses. He suggested that in addition to the explicit changes in the Reynolds stress transport equations, the higher order correlations were also changed. Irwin and Arnot Smith[4] have considered the Reynolds stress equations for small curvature together with the modified form of the Hanjalic and Launder[5] turbulence model, which uses three turbulent transport equations, for the shear stress, $\overline{u'v'}$, for the turbulent kinetic energy, $q^2/_2$, and for its dissipation rate. They concluded that the large effect of curvature could be accounted for by the extra terms that arise in the Reynolds stress equations and the turbulence model. Gibson et al.[6] removed the restriction of small curvature in their calculation method for turbulent boundary layers, using a turbulence model that contained the three normal Reynolds stress transport equations instead of just that for the turbulent kinetic energy. This work was extended to the curved two-dimensional wall jet by Gibson and Younis.[7] Launder and Rodi[8] have reviewed a number of turbulence models for use in wall jets, both Boussinesq eddy viscosity models and those using the Reynolds stress transport equations such as those mentioned above. An important feature of the effect of longitudinal curvature on a wall jet is that the outer layer, beyond the velocity maximum, is destabilized so that the turbulence is increased, while the inner or boundary layer flow is stabilized. In a plane wall jet the position of zero shear stress, y_s, is about 70 percent of the distance from the wall of the position of maximum velocity, y_m. The differential effect of curvature causes an increase in the difference between the values of y_s and y_m. No eddy viscosity model can predict this effect because the shear stress is related to the mean strain rate, and so the positions of zero shear stress and maximum velocity must coincide.

A large amount of experimental data has been gathered on plane and curved wall jets, much of which has been critically reviewed in an earlier paper by Launder and Rodi.[9] Much less attention has been paid to the effect of the strain rate due to divergence. Smits et al.[10] measured a boundary layer on a conical surface and concluded that the lateral divergence altered the turbulence structure in much the same way as longitudinal curvature. In reviewing experimental data on radial wall jets, Launder and Rodi[8] observed that the spreading rate is about 20 percent higher than that for plane wall jets with shear stress

Address reprint requests to Dr. Gregory-Smith at the School of Engineering and Applied Science, University of Durham, South Road, Durham, DL1 3LE, UK.

Received 12 April 1990; accepted 15 April 1991

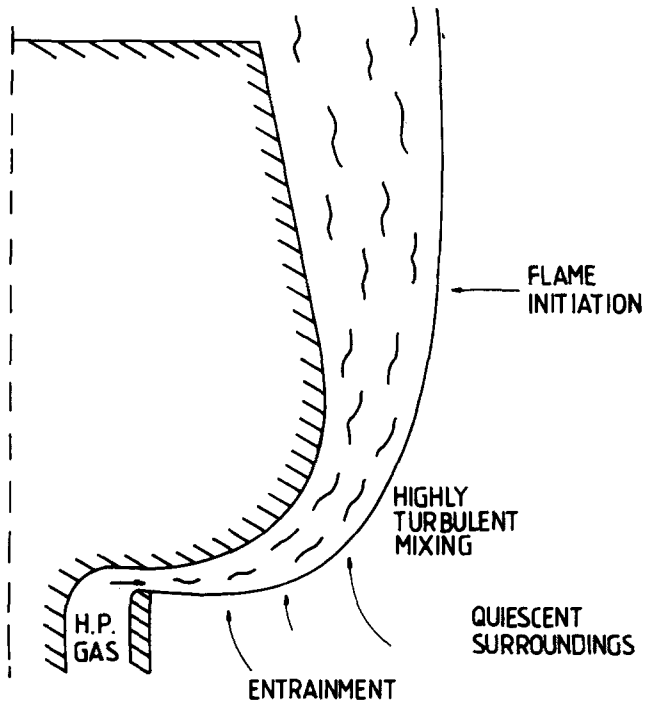

Figure 1 Principles of the Coanda flare

values about twice as high. Thus, with the Coanda flare geometry, where the jet has initially strong divergence as well as longitudinal curvature, the two rates of strain reinforce each other in the outer part of the jet, and very high turbulence may be expected.

While recognizing the shortcomings of the eddy viscosity model, Morrison and Gregory-Smith[11] presented a correction to the mixing length model for the effects of both divergence and streamwise curvature, appropriate to the Coanda flare geometry. Morrison[12] made measurements of mean velocities and Reynolds stresses in the jet on a model flare using hot-wire anemometry. Turbulence levels were much higher than in a plane wall jet, or in a wall jet over a cylindrical surface such as measured by Wilson and Goldstein.[13] The high levels of turbulence caused difficulties in making accurate measurements using hot-wire anemometry, and so some of Morrison's results are questionable.

Thus, a program of work was undertaken at the University of Durham with two aims. The first was to improve and extend the range of data for the jet over a Coanda flare using laser Doppler anemometry, which would be more accurate in regions of high turbulence. The second aim was to use the mixing length model of Morrison and Gregory-Smith to predict the jet development. The results of the modeling have been presented by Gregory-Smith and Hawkins,[14] and this paper presents the results of the laser Doppler measurements.

Apparatus

A closed loop water flow rig was used for the measurements. It operated with water that had been filtered from the mains supply through a 5-μ filter. This allowed sufficient small particles for natural seeding for the laser Doppler measurements. The circuit included a pump, an air-cooled radiator to maintain a near constant temperature of 20°C, a bypass to control the flow rate, and orifice plate metering upstream of the tank containing the model. The tank was constructed from 50-mm thick Perspex and had internal dimensions of 400 mm × 400 mm × 950 mm high.

The model consisted of a half-axisymmetric perspex piece, bolted onto a base plate, as shown in section in Figure 2.

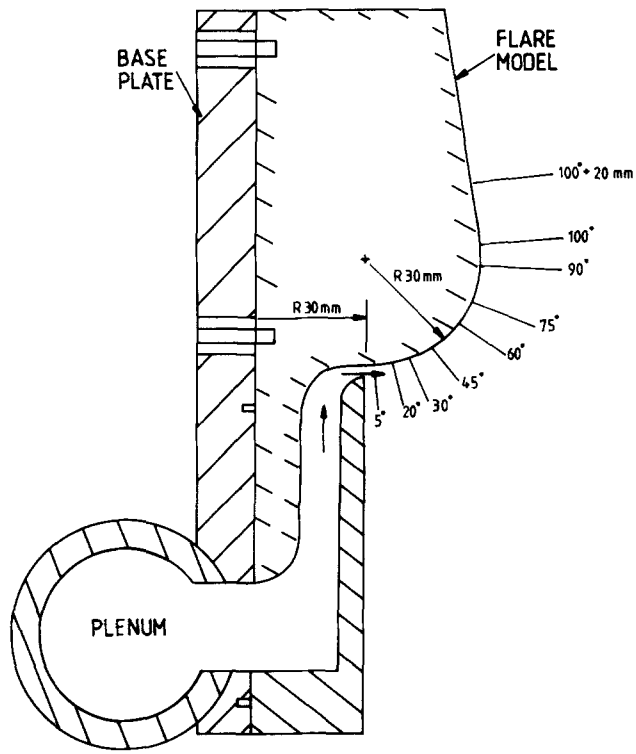

Figure 2 Model flare rig

Notation

a_1	Structural parameter for turbulence ($=\overline{u'v'}/q^2$)
Q	Jet mass flow rate
q_2	Twice the turbulent kinetic energy ($=\overline{u'^2}+\overline{v'^2}+\overline{w'^2}$)
R	Radius of longitudinal curvature of surface
t	Slot height
U, u'	Mean and fluctuating velocity component in streamwise direction
Um	Maximum streamwise velocity at given position along the flare surface
Us	Slot velocity
V, v'	Mean and fluctuating velocity component in radial direction
W, w'	Mean and fluctuating velocity component in circumferential direction
x, y, z	Streamwise, radial, circumferential coordinates
$y_{0.5}$	Normal distance from surface where $U = Um/2$
y_m	Normal distance where $U = Um$
y_s	Normal distance where shear stress becomes zero

Greek symbol

ξ	Dimensionless radial coordinate ($=y/y_{0.5}$)

Water entered the circular plenum chamber from the sides, before flowing to the slot and emerging as a jet into the surrounding water. Adjustment of the slot width was possible by movement of the model relative to the base plate. The slot width was 5 mm for this investigation, the streamwise radius of curvature of the surface was 30 mm, and the axisymmetric radius at the slot was also 30 mm. Traverses were made across the slot exit and at the angular locations around the curved section as shown in Figure 2. At 100°, the surface became conical, and a traverse 20 mm along the conical section was also made.

The L.D.A. system used a single beam argon-ion laser, with beam splitting and frequency shifting effected by a rotating diffraction grating. The system operated in forward scatter mode, with a commercial camera zoom lens used to project the image of the beam crossover onto a pinhole in front of a photomultiplier tube. The effective measuring volume size could be varied by adjusting the magnification of the zoom lens and altering the pinhole size. For this work a 50-μ pinhole was used, giving an effective measuring volume diameter of approximately 0.5 mm. This small volume allowed much finer resolution of the flow than is usually possible with hot-wire anemometry. Positional accuracy for each measuring point was estimated at 50 μ. The photomultiplier output signal was fed to a DISA 55L90a counter processor, and variable length windowing was achieved by a separate circuit, which controlled the ARM and INHIBIT lines on the counter. Data from up to 4,000 samples for a single reading were stored on a personal computer. The data was then transferred to a mainframe computer for analysis and graphical presentation.

Full details of the flow rig, model, and L.D.A. system are given by Hawkins.[15]

Experimental method

Hawkins and King[16] have reported a study of bias errors using the L.D.A. system to measure the flow in a sudden expansion of a circular pipe. An important conclusion was the need to ensure ergodic sampling by having a sampling period that was long compared with that for the lowest frequency present in the turbulence. The technique used for this Coanda jet flow study was described by Hawkins.[15] Details of the measurement procedure and data analysis were also given, and so only a brief description is given here.

Eight orientations of the beam cross-over were used for each measurement position. Four of these, at 45° intervals, were in the streamwise/radial (x, y) plane, and four in the radial/circumferential (y, z) plane. These measurements provided data redundancy for the three mean velocity components and five of the six Reynolds stresses. A least-squares fitting technique was used, which also gave a confidence interval for each quantity. The missing stress is $\overline{u'w'}$ (streamwise/circumferential), which should be zero in axisymmetric flow. The profiles presented here result from a least-squares spline fit, with weightings being proportional to the confidence intervals. An example at the 90° position is shown in Figure 3, where the intervals correspond to a confidence limit of 95 percent.

A number of measurements were made to check the axisymmetry of the flow. Two traverses along the 90° line of latitude were made, one at 4 mm from the surface, the other at 10 mm. Data was collected at 1° intervals to 5° either side of the center line. Typical results are shown in Figure 4, which shows the mean velocities and three of the Reynolds stresses at the 4-mm distance. As can be seen, there is some fluctuation in values, but they are fairly small and show no consistent trend, either from one side to the other or periodically. For boundary layers destabilized by concave curvature, longitudinal (Taylor-Görtler) vortices have been observed, e.g., Smits et al.[10] However, these

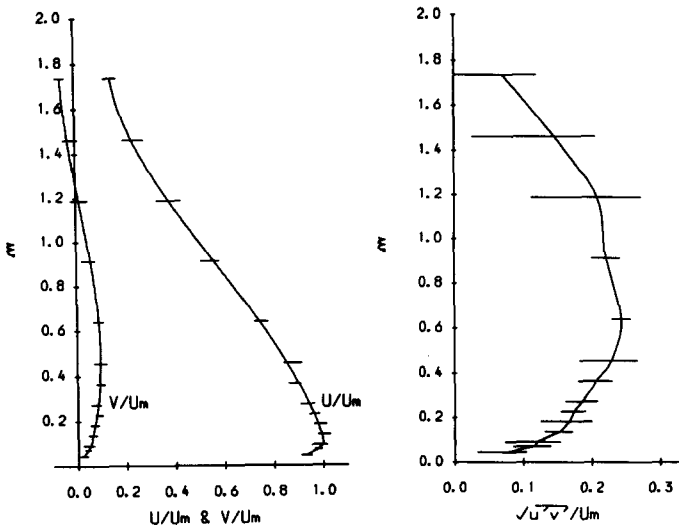

Figure 3 Confidence intervals and curve fits at 90°

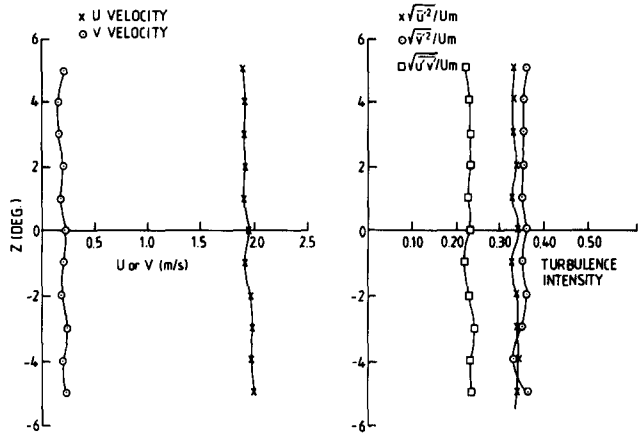

Figure 4 Variation with circumferential position at 90°

have not been widely observed in wall jets over convex surfaces, although in studying flow over a full-scale Coanda flare, Senior[17] has reported surface oil streaks on the conical section, perhaps caused by longitudinal vortices. The streaks were at angular displacement of about 10°, and so the 10° extent of the circumferential traverses (equivalent to 1.1 $y_{0.5}$) should have indicated some periodicity due to longitudinal vortices if they were present. Full radial traverses were also performed on either side of the center line. For example, the mean W (circumferential) velocity was taken at 45° either side of the center line. The W velocity should, of course, be zero for axisymmetric flow, and it was found to be always less than 5 percent of the maximum streamwise velocity at this position. The $\overline{v'w'}$ shear stress was also very small for all the traverses.

The checks described above, together with comprehensive precautions to ensure the quality of the manufacture of the model, gave confidence that the flow was acceptably axisymmetric. Ideally, a momentum balance should have been carried out, since, as Launder and Rodi[9] point out in their review of turbulent wall jets, this is a more rigorous test of two-dimensionality than is the inspection of velocity profiles. However, it was not possible to adopt such a refinement in this survey due to the absence of pressure measurements, which would be required in this curved flow situation.

As indicated above, traverses were made radially outward from the surface at the locations shown in Figure 2. However, the geometry of the rig did not allow the four measurements

in the (y, z) plane to be made for angular values of less than 60°. Thus, for those positions, no values of the circumferential normal stress ($\overline{w'^2}$) or mean velocity (W) were obtainable. For presentation of velocity and Reynolds stress profiles, the results were made dimensionless with respect to the maximum streamwise velocity, Um, at that location. The radial distance from the surface was expressed as $\xi = y/y_{0.5}$ where $y_{0.5}$ is the distance corresponding to $U/Um = 0.5$. The traverses were conducted at a slot Reynolds number of 4.2×10^5, corresponding to a slot velocity of 4.2 m/sec.

Jet development

The development of the jet is shown in Figures 5 and 6. Figure 5 shows the growth of $y_{0.5}$ and the changes in the relative positions of the maximum velocity, y_m, and the zero shear stress, y_s. At the slot the radial outflow of the jet causes it to thin initially, before entrainment causes it to grow increasingly rapidly. At a value of $x/t = 10.5$, the 100° position is reached, and the jet growth rate decreases thereafter as the streamwise curvature is removed. The values of y_m and y_s were not determined very accurately, and there is some scatter in the results. However, it appears that the ratio of y_m to $y_{0.5}$ increases rapidly at first, and then less so, while the ratio of y_s to $y_{0.5}$ falls rapidly to a minimum of $x/t = 10.5$ where the streamwise curvature ends, and then rises slightly along the conical surface. In Figure 6, the maximum velocity shows an initial rise as the curvature of the flow produces a subambient pressure on the surface, followed by a reduction due to the increasing mass flow. A further indication of the jet development is given by the increase in mass flow in the jet (obtained by integrating the velocity profiles) as shown also in Figure 6. The mass flow increase is roughly linear with distance, in contrast to the plane wall jet, which increases proportionally to $\sqrt{x/t}$. This indicates the increase in entrainment caused by the divergence and streamwise curvature.

The streamwise and radial mean velocity profiles are shown in Figures 7 and 8. The U velocity profiles at the slot and 5° positions are fairly flat topped as might be expected. However by 20°, the outer shear layer has grown so rapidly that the profiles from there on look fairly similar. By contrast, the V profiles show no tendency toward similar profiles other than radial outflow in the inner part of the jet as the maximum velocity decays, and inflow in the outer part where entrainment is taking place. The profile at the slot shows unexpectedly large inflow, which is discussed later. It should be noted that the symbols in Figures 7 and 8 (and the subsequent plots, Figures 9–12) are not data points, but are for identification only. As stated above, the curves are best fits to the data (see Figure 3).

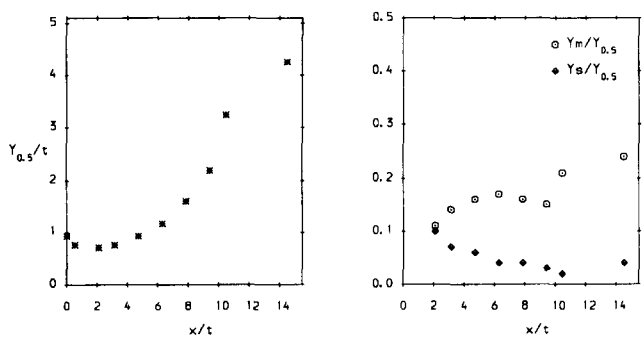

Figure 5 Jet growth

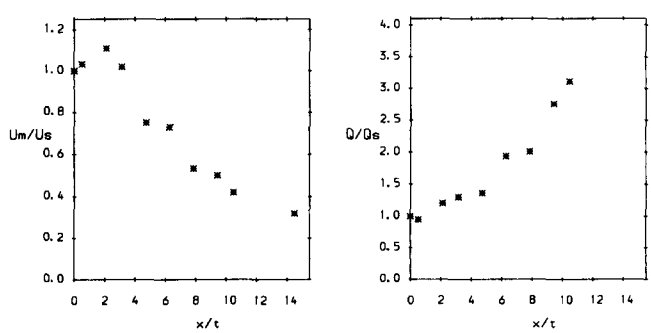

Figure 6 Velocity decay and entrainment rate

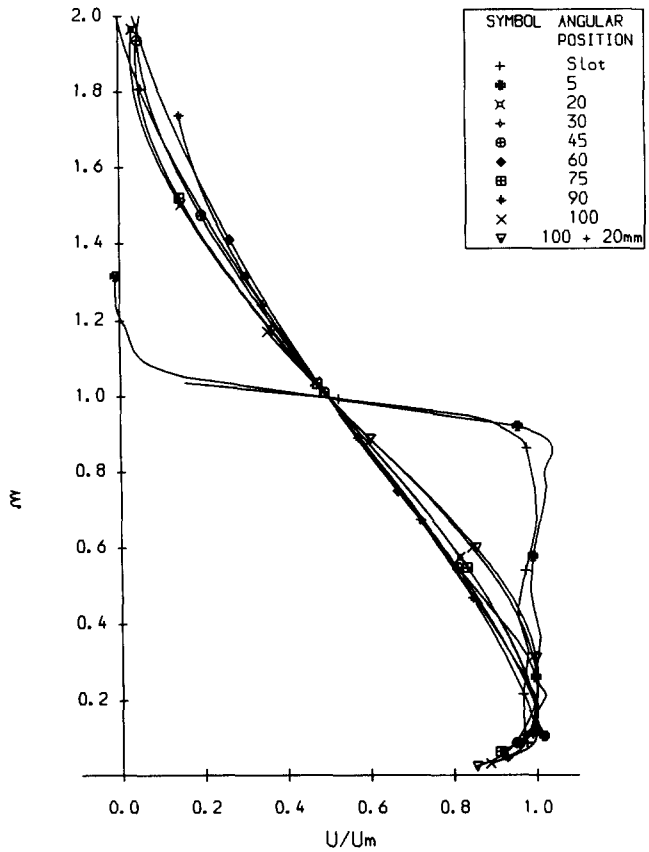

Figure 7 Mean streamwise velocity profiles

Normal stresses are shown in Figures 9–11 expressed as rms turbulence intensities relative to maximum velocity. In Figure 9, the streamwise intensities for the slot and 5° locations show a peak coinciding with the position of high negative velocity gradient, giving high generation of turbulence there. The intensities rise rapidly around the curved surface, with profiles for 45° and beyond being fairly similar. The turbulence intensity reaches a maximum at 75°, drops at 90°, but rises again at 100° and 100° + 20 mm positions. Generally, the values are fairly constant over the jet width out to $\xi = 0.9$, decreasing further out. However, when Figure 9 is read with Figure 7, it can be seen that the local turbulence intensities become very high indeed in the outer part of the jet.

In Figure 10 the radial intensities are shown. Their behavior is very similar to the streamwise values, except for the very marked suppression of turbulence inboard of $\xi = 0.4$, due to the proximity of the surface. Figure 11 shows the circumferential intensities, but as explained above, only for the last four locations. They show similarity to the streamwise values, with a slight rise as the surface is approached. The marked rise close to the surface for 100° may be somewhat exaggerated by the curve-fitting technique.

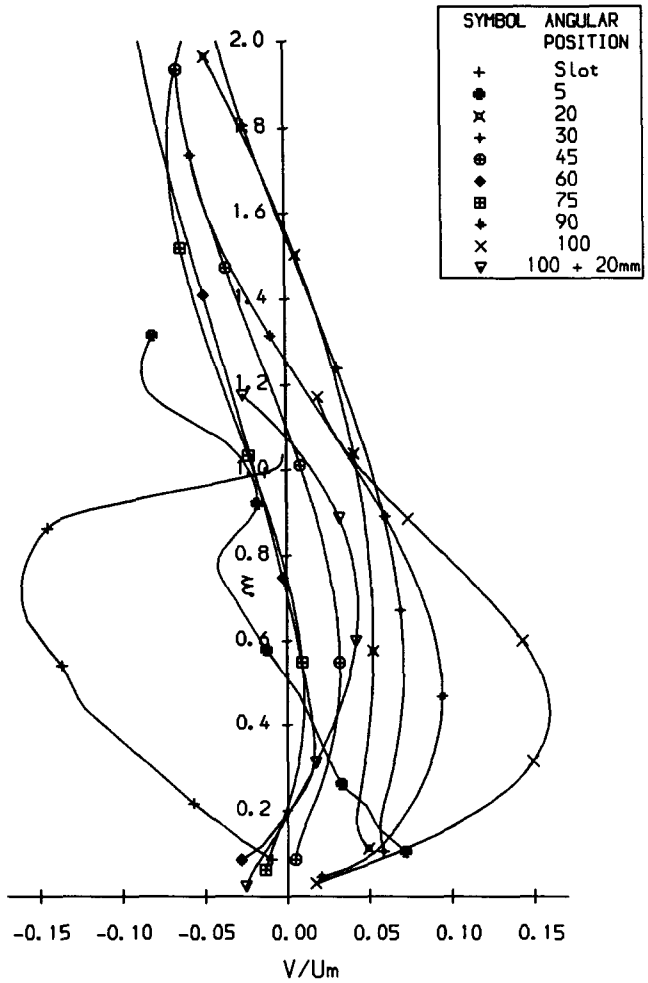

Figure 8 Mean radial velocity profiles

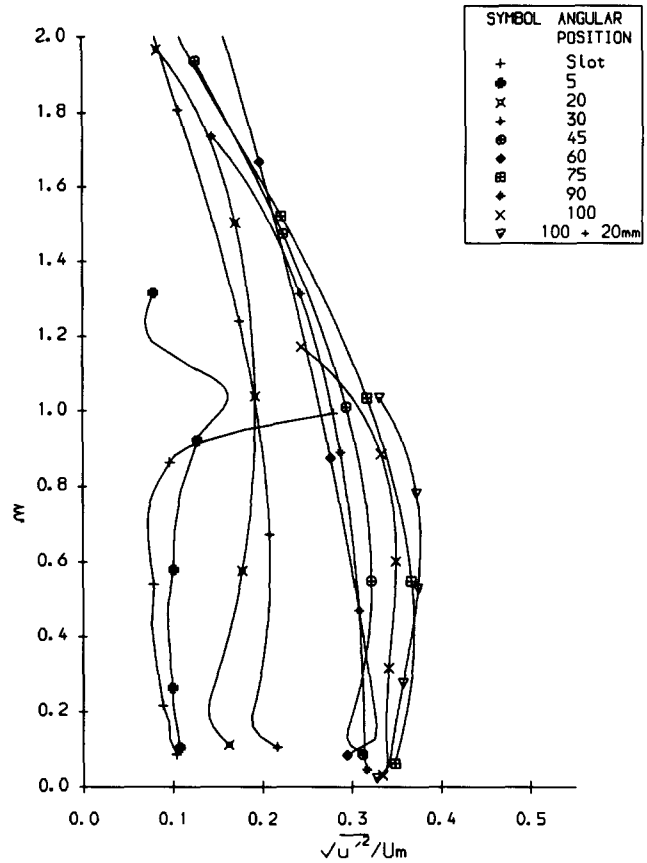

Figure 9 Streamwise turbulence intensities

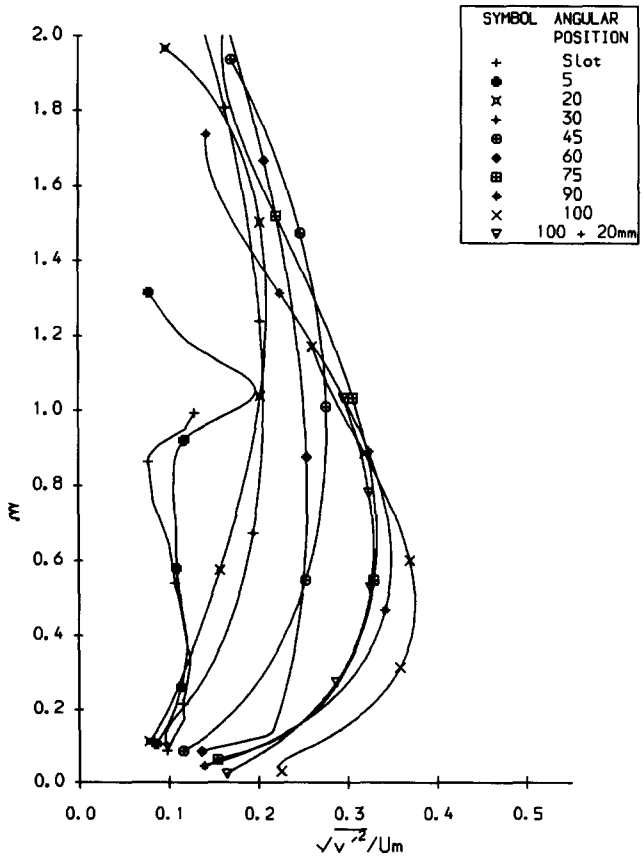

Figure 10 Radial turbulence intensities

The shear stress correlation, $\overline{u'v'}/Um^2$, is shown in Figure 12. For the slot and 5° locations the values are low, except at the edge of the jet, where the large velocity gradient causes high turbulence as seen in Figures 9 and 10. Thereafter, the values rise rapidly around the surface to give fairly similar values for 45° and beyond. However, there seems some inconsistency at the 60° location, which is lower than both the 45° and 75° profiles. The highest values are seen at 75°, with a reduction at 90°, followed by a slight increase at 100° and then decrease at 100° + 20 mm as the curvature is removed.

Discussion

The initial thinning of the jet and rise in maximum velocity are expected, as indicated above. For an inviscid jet at the 20° position, the value of $y_{0.5}/t$ would be 0.73, and Um/Us would be 1.12, which are fairly close to the observed values in Figure 5. However, as Figure 7 shows, by 20° the viscous shear layer has completely eroded the potential core, and so one would expect less thinning and a lower maximum velocity than for the inviscid jet. Figure 8 shows large inflow velocities at the slot exit plane, due probably to the shape of the passage upstream. Thus it appears there is a vena contracta effect taking place downstream of the slot, causing additional thinning and rise in maximum velocities. This implies that as far as the later jet development is concerned, the effective slot width is somewhat less and the effective slot velocity somewhat greater than their physical values.

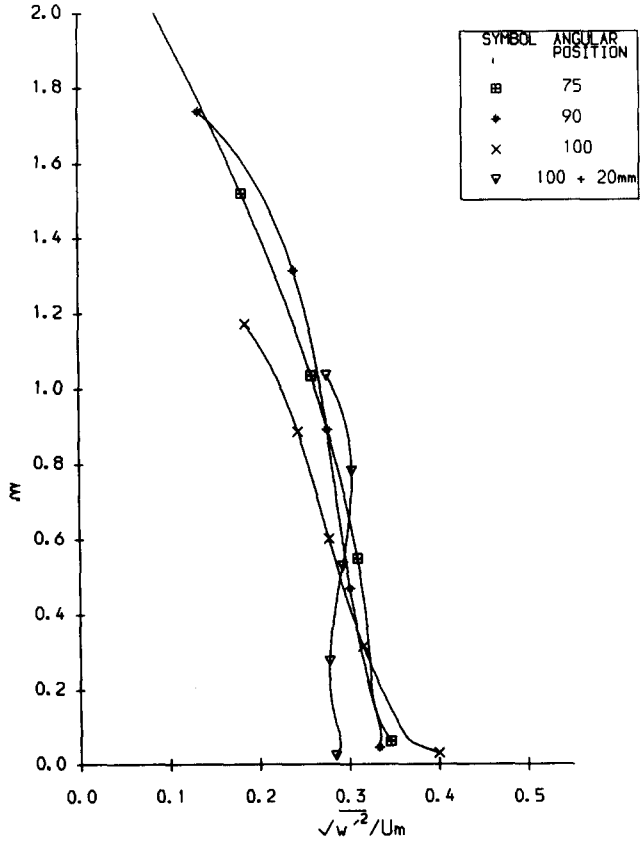

Figure 11 Circumferential turbulence intensities

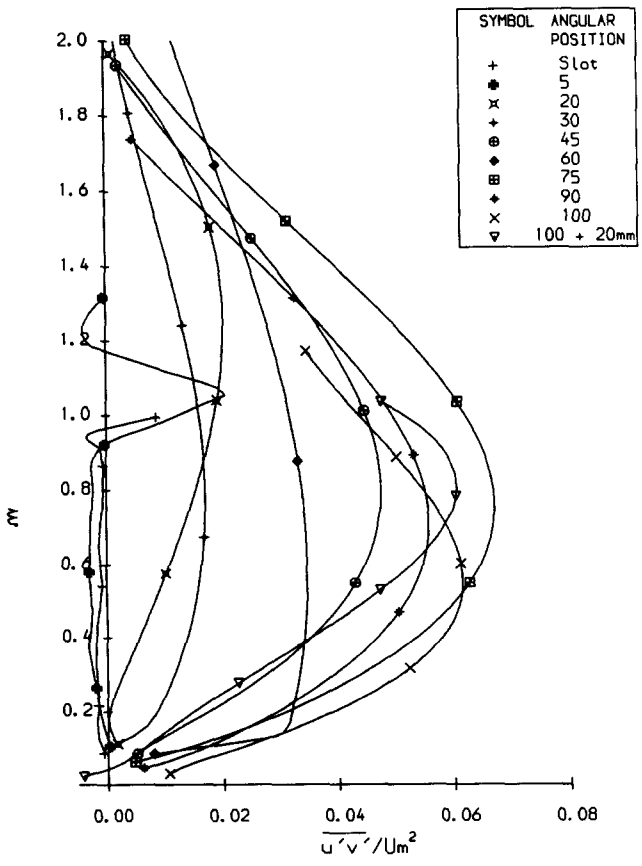

Figure 12 Shear stress profiles

The separation of the positions of maximum velocity and zero shear is very dramatic, as seen in Figure 5. The value of $y_m/y_{0.5}$ rises from 0.11 at the 20° position to 0.24 on the conical section. This compares with a value of around 0.15 given in the review of Launder and Rodi[9] of plane wall jet data. For wall jets over log spiral surfaces they give a correlation

$$y_m/y_{0.5} = 0.159 + 0.205 y_{0.5}/R$$

This would suggest values of 0.188 at 20° and 0.292 at 100° for the corresponding $y_{0.5}/R$ values for the Coanda flare surface. For cylindrical surfaces, the available data is generally for much milder curvature ($t/R = 0.05$ or less compared with 0.2 for this work). However, a recent paper by Fujisawa and Kobayashi[18] gives results for a wall jet on a plane followed by a cylindrical surface. For their case of $y_{0.5}/R = 0.15$ at $\theta = 0°$, the value of $y_m/y_{0.5}$ is 0.14 at $\theta = 22.5°$, rising to 0.18 at $\theta = 12.5°$. Data for the position of zero shear stress is not widely available, although Wilson and Goldstein[13] show a value for $y_s/y_{0.5}$ of 0.1 for a plane wall jet, which is the same as the value at 20° in this work. Their Figure 8 shows very small values for their cylindrical surface with $t/R = 0.03$, but these are not quantified. For a much smaller t/R value of 0.003, Alcaraz et al.[19] give values for $y_s/y_{0.5}$ of 0.077 at $\theta = 5°$, reducing to 0.050 at $\theta = 16°$. Figure 5 shows qualitative agreement with Alcaraz et al., with $y_s/y_{0.5}$ decreasing rapidly on the curved surface of the Coanda to a minimum of 0.02, and then showing an increase as the surface curvature is removed. The ratio of the strain rate due to divergence to that due to curvature at $y = y_{0.5}$ falls from approximately 1.02 at $\theta = 5°$, to 0.45 at $\theta = 45°$, to zero at $\theta = 90°$. Thus, the strong divergence of the jet close to the slot should destabilize not only the outer layer but also the inner layer, countering the stabilizing effect of longitudinal curvature on the inner layer. This may explain the relatively high starting value of $y_s/y_{0.5}$ seen in Figure 5.

Guitton and Newman[20] showed that a wall jet flowing over a logarithmically curved spiral surface should be self-preserving if the skin friction coefficient is effectively constant. This results in a wall jet whose ratio of $y_{0.5}/R$ is constant along the surface. Clearly, the Coanda flare jet cannot be expected to be self-preserving. However, Wilson and Goldstein[13] observed that on their cylinder the wall jet (which also is not self-preserving) appeared to give fairly similar streamwise velocity profiles. This is also seen for the Coanda wall jet in Figure 7, and is in marked contrast to the expected lack of similarity shown by the normal velocity (Figure 8) and the Reynolds stresses (Figures 9–12). Wilson and Goldstein reasonably state, "The apparent similarity of the mean velocity profile must be regarded as an indication of its insensitivity to departures of the entire velocity field from self-preservation."

The effects of the divergence and curvature on the flow are very noticeable in the profiles of the Reynolds stresses shown in Figures 9–12. The normal and shear stresses are typically two to three times higher than those for the plane wall jet given by Wilson and Goldstein.[13] The values are also much higher than those for their curved jet, or for the thicker curved jet of Fujisawa and Kobayashi.[18] For instance Figure 13 shows the maximum values of streamwise turbulence intensity plotted against jet half-width to radius ratio, $y_{0.5}/R$, with the range of data from the above curved jets. A rapid rise in maximum values is seen where the divergence effect is present, and then they level off as the divergence reduces and finally becomes slightly negative at the 100° position (the 100° + 20 mm point is not included). The divergence and curvature effects are also seen in the very rapid growth of the outer shear layer downstream of the slot as it encroaches completely into the potential core after two slot heights (corresponding to 20°). In a plane wall jet this distance is between five to ten slot heights.

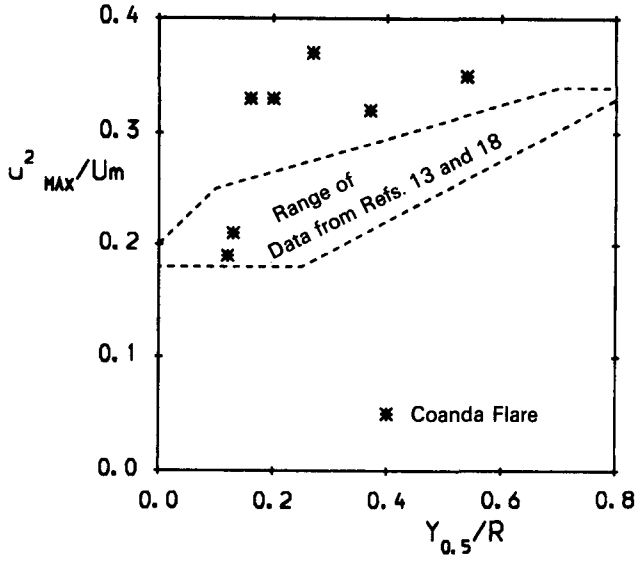

Figure 13 Maximum streamwise turbulence intensities

A comparison with the data of Morrison[12] shows that the results presented here show a much greater degree of consistency, although values are generally similar. For instance, Morrison and Gregory-Smith[11] show that at 100°, the values of $\overline{u'v'}/Um^2$ rise steadily to about 0.06 at $\xi = 1.0$, but then show a sudden jump to around 0.11 in the outer part of the jet, whereas Figure 12 shows a smoother variation up to a maximum of around 0.06, and then a decline.

Wilson and Goldstein[13] cite Bradshaw et al.[21] and Hanjalic and Launder[5] whose turbulence modeling related shear stress to turbulent kinetic energy. The suggestion was that some degree of self-preservation may be apparent for nonequilibrium turbulent flows if turbulence parameters are scaled relative to each other rather than to the maximum velocity scale Um. They showed, however, by plotting the parameter $a_1 = \overline{u'v'}/q^2$, that the nonequilibrium nature of their curved wall jet was still shown. A comparable plot for the present study is shown in Figure 14, and it appears similar to that of Wilson and Goldstein. The values rise as the jet develops around the surface, with consistently high values for 60° to 100°. Removal of the streamwise curvature appears to cause a drop in values for the 100° + 20 mm location. The figure confirms the conclusion of Wilson and Goldstein that the nonequilibrium nature of the jet is still apparent using this type of scaling.

Although only one position was traversed on the conical section after the removal of the longitudinal curvature, there are indications of a return to the conditions expected in a plane wall jet. Figure 5 shows a reduction in the rate of growth and an increase in the value of $y_s/y_{0.5}$. A fuller streamwise profile for the 100° and 100° + 20 mm positions is seen in Figure 7, and there is a rapid reduction in the radial outflow in Figure 8 after 100°. A reduction in the levels of normal turbulence intensity (Figure 10) and shear stress (Figure 12) are also seen after 100°, although the streamwise and circumferential intensities (Figures 9 and 11) do not show a general reduction. Clearly traverses further downstream would be required to see whether the conditions returned monotonically to those for a jet along a cylindrical or conical body. Smits et al.[10] have observed nonmonotonic behavior after the removal of destabilizing concave curvature on a boundary layer, with a reduction of shear stress values below plane boundary layer values after about ten boundary layer thicknesses. The 20-mm position along the conical section is roughly equal to the half-width,

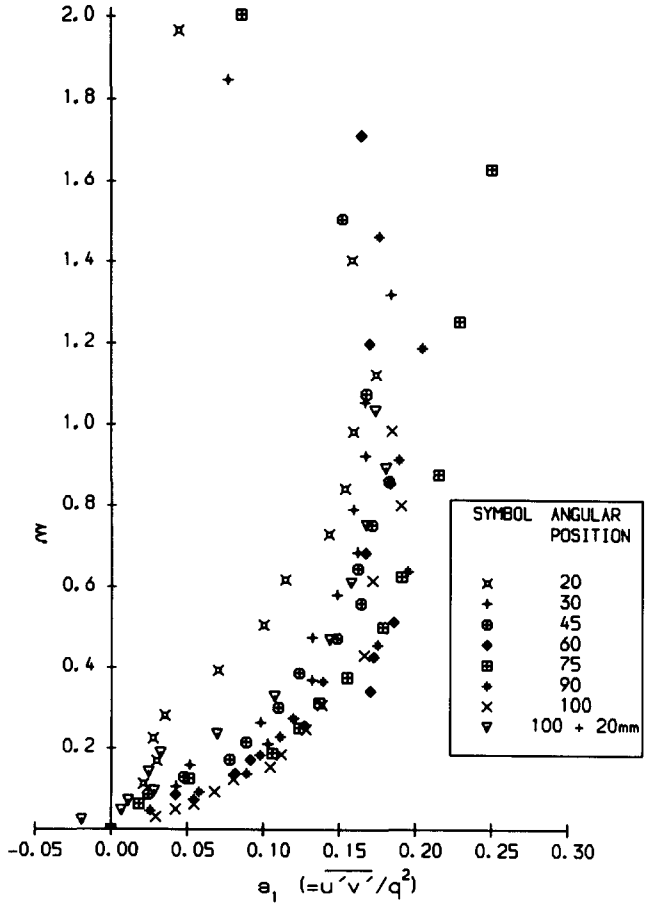

Figure 14 Structural parameter profile

$y_{0.5}$, of the jet, and so the effects of removal of curvature have not had time to become fully apparent.

As regards the isotropy of the turbulence, inspection of Figures 9–11 show that the outer part of the jet has generally very similar values of the three turbulence intensities. The most noticeable feature is the suppression of the radial component, $\overline{v'^2}$, near the surface. In the outer part of the jet the radial value is generally the highest of the three over the curved portion of the surface. This results from the curvature enhancing primarily the radial fluctuations of turbulence. On the conical portion at 100° + 20 mm, the radial component drops below the streamwise component of turbulence as the curvature is removed.

The eddy viscosity (made dimensionless with respect to Um and $y_{0.5}$) is shown in Figure 15. The values are shown in the outer part of the jet only, as they go through infinity at the velocity peak. In fact, the curves for 100° and 100° + 20 mm seem to be heading that way. The range of values may be compared with a maximum of 0.025 given by a standard K-epsilon model presented by Gregory-Smith and Hawkins.[14] They also presented values given by the mixing length model of Morrison and Gregory-Smith,[11] modified for this type of flow. The modified mixing length model gave similar levels of eddy viscosity to those observed here.

Conclusions

A single component laser Doppler anemometer has been used to map the highly turbulent flow field produced by an axisymmetric curved wall jet. Consistent results of quantifiable accuracy have been obtained for the mean velocities and five of the six Reynolds stresses. The missing stress is the streamwise-circum-

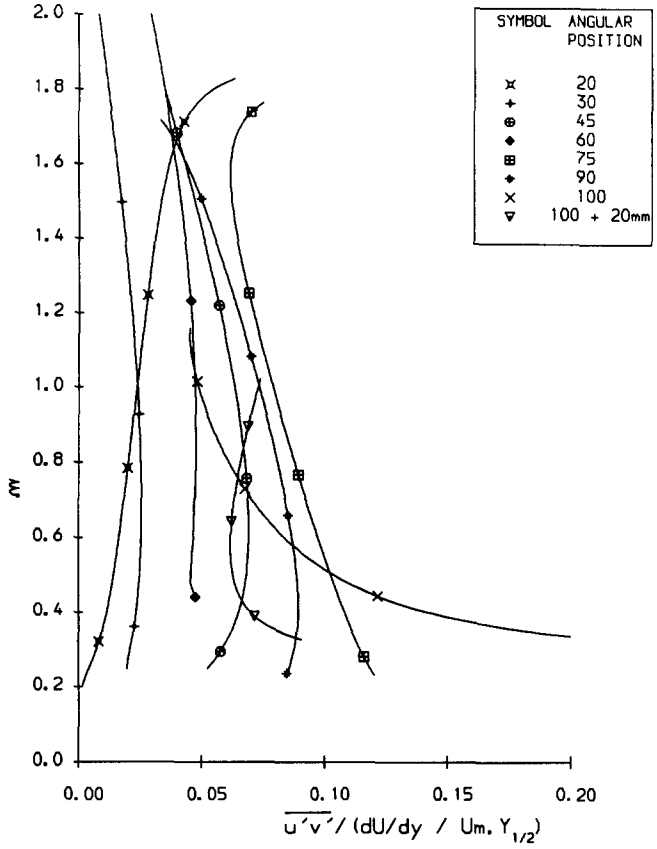

Figure 15 Eddy viscosity profiles

ferential component, which should be zero in this axisymmetric flow. Care was taken to ensure axisymmetry of the flow, and checks showed that the flow was acceptably axisymmetric, with no evidence of streamwise vortices that have been observed for boundary layers destabilized by concave curvature.

The divergence and streamwise curvature results in extra rates of strain acting on the flow, and is evidenced by several phenomena:

(1) high turbulence intensities;
(2) high streamwise-radial shear stress and eddy viscosity;
(3) enhanced separation of positions of maximum velocity and zero shear stress;
(4) high rate of entrainment;
(5) lack of attainment of self-preservation.

The removal of streamwise curvature and the slight convergence of the flow downstream results in a generally monotonic return of the jet toward conditions expected of a plane wall jet. However, this work has not studied exhaustively the effect of the removal of curvature in this situation. To give a more complete picture, further measurements along the conical portion of the flare are required.

A limitation of this work stems from the design of the passage upstream of the slot. The design was modeled from a full-scale Coanda flare, but it appears to result in nonparallel flow at the slot exit and a downstream vena contracta. This probably affects the near jet development, which is very rapid, and so further investigation is warranted. However, the effect on the later structure of the jet is likely to be minimal, altering only the effective slot height and exit velocity. A further, although not serious, limitation is the inability to measure circumferential components of the flow for angles less than 75°.

A major development of this work would be to the internal Coanda jet, i.e., where the jet flows inward toward the axis of symmetry around the inside of a trumpet-shaped channel. Such convergent flow would reverse the sign of the strain due to divergence and should result in reduced levels of turbulence. This would also extend the applicability of the work to such devices as air movers and Coanda-type ejectors. On the theoretical and computational side, this work provides accurate data for the development and testing of turbulence models that should allow for the extra rates of strain present in this flow.

Acknowledgment

The authors gratefully acknowledge the support of the Science and Engineering Research Council for this work.

References

1 Bradshaw, P. Effects of streamline curvature on turbulent flow. *AGARDOgraph*, **169**, 1973
2 Bakke, P. Experimental investigations of a wall jet. *J. Fluid Mech.*, 1957, **2**, 467
3 Wilkins, J., Witheridge, R. E., Desty, D. H., Mason, J. T. M., and Newby, N. The design, development and performance of Indair and Mardair Flares. *9th Ann. Offshore Tech. Conf.*, Houston, 1977, 2822
4 Irwin, H. P. A. H., and Arnot Smith, P. Prediction of the effect of streamline curvature on turbulence. *Phys. Fluids*, 1975, **18**, 624
5 Hanjalic, K., and Launder, B. E. A Reynolds stress model of turbulence and its application to thin shear flows. *J. Fluid Mech.*, 1972, **52**, 609
6 Gibson, M. M., Jones, W. P., and Younis, B. A. Calculation of turbulent boundary layers on curved surfaces. *Phys. Fluids*, 1981, **24**, 386
7 Gibson, M. M., and Younis, B. A. Modelling the curved turbulent wall jet. *AIAA*, 1982, **20**, 1707
8 Launder, B. E., and Rodi, W. Turbulent wall jet—measurement and modelling. *Ann. Rev. Fluid Mech.*, 1983, **15**, 429
9 Launder, B. E., and Rodi, W. The turbulent wall jet. *Prog. Aerospace Sci.*, 1981, **19**, 81
10 Smits, A. J., Young, S. T. R., and Bradshaw, P. The effect of short regions of high surface curvature on turbulent boundary layers. *J. Fluid Mech.*, 1979*a*, **94**, 209
11 Morrison, J. F., and Gregory-Smith, D. G. Calculations of an axisymmetric turbulent wall jet over a surface of convex curvature. *Int. J. Heat and Fluid Flow*, 1984, **5**, 139
12 Morrison, J. F. Axisymmetric wall jet with streamline curvature. Ph.D. Thesis, Durham University, UK, 1982
13 Wilson, D. J., and Goldstein, R. J. Turbulent wall jets with cylindrical streamwise curvature. *J. Fluids Eng.*, 1976, **98**, 550
14 Gregory-Smith, D. G., and Hawkins, M. J. Modelling an axisymmetric curved wall jet with application to the Coanda flare. *Proc. 3rd. Int. Phoenics User Conf.*, Dubrovnik, Yugoslavia, 1989
15 Hawkins, M. J. A study of turbulent flows and curved jets including the application of the laser doppler anemometry technique. Ph.D. Thesis, Durham University, UK, 1988
16 Hawkins, M. J., and King, C. F. L.D.A. studies in a sudden expansion water flowrig. *Proc. Int. Conf. on L.A. Advances and Applications*, 1987, 28
17 Senior, P. The aerodynamics of curved jets and breakaway in Coanda flares. Ph.D. Thesis, University of Durham, UK, 1991
18 Fujisawa, N., and Kobayashi, R. Turbulence characteristics of wall jets along strong convex surfaces. *Int. J. Mech. Sci.*, 1987, **29**, 311
19 Alcaraz, E., Charnay, G., and Mathieu, J. Measurements in a wall jet over a convex surface. *Phys. Fluids*, 1977, **20**, 203
20 Guitton, D. E., and Newman, B. G. Self-preserving turbulent wall jets over convex surfaces. *J. Fluid Mech.*, 1977, **81**, 155
21 Bradshaw, P., Ferris, D. H., and Atwell, N. P. Calculation of boundary-layer development using the turbulent energy equation. *J. Fluid Mech.*, 1967, **28**, 593